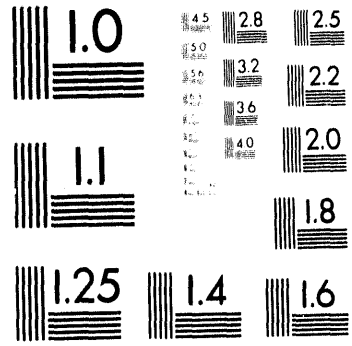
1.0
1.1
1.25
1.4
1.6
1.8
2.0
2.2
2.5
2.8
3.2
3.6
4.0
4.5
5.0

1 of 1

UCRL-JC-111337
PREPRINT

Shock Sensitivity of IHE at Elevated Temperatures

P. A. Urtiew
T. M. Cook
J. L. Maienschein
C. M. Tarver

This paper was prepared for submittal to
Tenth International Detonation Symposium, Boston, MA
July 12-16, 1993

June 1993

SHOCK SENSITIVITY OF IHE AT ELEVATED TEMPERATURES

P. A. Urtiew, T. M. Cook, J. L. Maienschein and C. M. Tarver
Lawrence Livermore National Laboratory
Livermore, California 94550

Insensitive high explosives (IHE's) based on triamino-trinitrobenzene (TATB) have been demonstrated to be very insensitive to shock, thermal, friction and other stimuli. Hazard scenarios can involve more than one one stimulus, such as heating followed by fragment impact (shock). The shock sensitivity of the IHE's LX-17 and PBX-9502 preheated to a temperature (250°C) just below thermal runaway is quantitatively studied using embedded manganin pressure gauges. The thermal expansion of TATB to 250°C is measured to determine the state of the explosive prior to shock initiation. LX-17 and PBX-9502 are found to be significantly more sensitive at 250°C than at lower temperatures, but still less sensitive than ambient temperature HMX-based explosives. An ignition and growth reactive flow computer model of the shock initiation of hot IHE is developed to allow predictions of the response of hot IHE to impact scenarios which can not be tested directly.

INTRODUCTION

With safety issues playing a dominant role in the present-day energetic materials technology, concern is growing about the safety of explosives exposed to extreme environmental conditions. In particular, this concern is expressed regarding so-called insensitive high explosives (IHEs), which normally are very insensitive to shock and other threatening initiation stimuli. However, when such an IHE is exposed to heat, it may become more sensitive to impact or to any other initiation mechanism.

Previous experiments[1,2] with the TATB-based explosive LX-17,* have shown that it indeed does become more sensitive to shock but may still be regarded as an IHE when compared to other HMX-based conventional HEs. Recently, experiments at Los Alamos[3] showed that IHE (PBX-9502**) and LX-17 not only become more sensitive to impact at 250°C but become nearly as sensitive as the conventional PBX 9404*** when plotted on the run distance to detonation vs impact pressure plot usually called the "Pop-plot".[4]

---

* TATB/Kel-F 800 (92.5/7.5)
** TATB/Kel-F800 (95/5)
*** HMX/NC/CEF (94/3/3)

Because of the important impact these observations may have on the accepted view of IHE and overall safety of various explosives systems, new experiments were undertaken to compare the results obtained by other techniques. This attempt to obtain more detailed information on the behavior of IHE under severe thermal environmental conditions formed the basis for this investigation. The main objectives here are to determine the impact thresholds for LX-17 and PBX-9502 heated to 250°C, to determine rates below the thresholds for detonation and to develop a reactive flow computer model for predictions of shock initiation of hot IHE's in untestable scenarios.

THERMAL EXPANSION OF LX-17

To characterize the behavior of heated IHE under dynamic loading, it is very important to know its physical state at high temperature before it is shocked. Measurements were made of the static thermal expansion of LX-17 up to 290°C, since the literature data do not extend beyond 100°C.[5-7] Pellets of LX-17, with length/diameter of 8.5 mm/4.4 mm or 2.9 mm/8.7 mm, were uniaxially pressed; these dimensions were chosen to give a wide range of the length/diameter (L/D) ratio. Most pellets were pressed at 20°C, and had densities of ≈ 1.89 g/cc (97.4% TMD). Thermal expansion was measured in the axial (i.e. along the axis of the cylinder) and radial (i.e.. from center to edge of cross-section of cylinder) directions for both L/D ratios; from this, the coefficient of thermal expansion (CTE) and density were calculated. Thermal expansion measurements were made with a DuPont 941 Thermal Mechanical Analyzer (TMA) which was controlled by a DuPont 990 Thermal Analyzer, with an accuracy of ±3% of the actual reading. Expansion measurements were made at a heating rate of 5°C/minute. More detail on sample preparation and further experimental results are given by Maienschein.[8]

Axial and radial growth data for cold-pressed LX-17 pellets are shown, as percent of initial length, in Figure 1. The axial expansion is, on average, 55% greater than the radial expansion. The thermal expansion of crystalline TATB perpendicular to the aromatic ring is ≈ 30 times larger than thermal expansion in the plane of the aromatic ring,[5] so the enhanced axial expansion of LX-17 indicates partial orientation of the TATB crystals, with the aromatic ring being forced perpendicular to the axis along which compaction pressure is applied.

Samples with both L/D ratios are included in Figure 1. If thermal expansion were driven by gas bubbles evolving in the LX-17, the axial and radial expansions would be different for different L/D ratios.[8] However, the results were indistinguishable for the two L/D ratios, so all data were combined in one plot.

The CTEs in the axial and radial directions are given by the derivatives of the data in Figure 1. Using the second-order polynomials shown in Figure 1, the CTEs are (in units of 10^{-6} m/m/°C):

$$CTE_{axial} = 117 + 0.420\ T \qquad (1)$$

and

$$CTE_{radial} = 92.4 + 0.161\ T \qquad (2)$$

where T is temperature in °C. The volumetric CTE is given by:

$$CTE_{volumetric} \approx 2*CTE_{radial} + CTE_{axial} \quad (3)$$

The resultant CTE values are shown in Figure 2, along with literature data (at lower temperatures). One may note that use of a different function to fit the expansion data will give a different dependence of CTE on temperature; however, in the absence of a physical model the simplest function that fits well (i.e. 2nd-order polynomial) is suitable. The volumetric CTE reported by Kolb[5] is reasonably consistent with the present data, but the other literature data[6,7] are lower than these results.

It was observed that, for pellets pressed at 100°C, additional expansion above that shown in Figure 1 occurred as the sample passed from 70 to 140°C. The higher density of hot-pressed pellets is apparently achieved by freezing extra strain into the solid, and this strain is released during thermal cycling. Calculation of CTEs for hot-pressed LX-17 is discussed by Maienschein.[8]

DYNAMIC TESTS

In contrast to other experiments, which provide data only on shock and detonation velocity, the present approach is to do the experiments in the 4-in. smooth-bore gas gun, which will provide much more detailed information on pressure variation within the heated sample. The 4-in. gun thermal experiment is illustrated in Figure 3. Here, the target is much more complex than usual because it must contain not only the thin foil manganin gauges to measure dynamic changes of pressure but also two nichrome heaters to heat up the sample and eight thermocouples to monitor the temperature. All the placements within the target have to be thin and properly bonded to provide a unit without voids and with the least amount of dynamic impedance mismatch. All components such as adhesives, Teflon armor, solder joints, and signal cables had to be checked separately for strength and compatibility to withstand a full thermal load of 250°C. The gauges themselves had to be checked as well under the heated environment to make sure that they operate properly and respond to pressure as they do under ambient conditions.

A typical gas gun experiment with IHE is illustrated in Figure 4. Here a target assembly is shown in (a) before and after heating. With the aluminum back plates fixed at the target holder, IHE is allowed to thermally expand towards the impact surface. Locations of the gauge stations are also shown in (a). The waves generated by the impact of the projectile with the target is shown on the time distance plot in (b). Here the shock waves are represented as solid lines, particle motion as broken lines and rarefaction waves as chain dotted lines. The zero time on this plot is taken as the time the projectile strikes the crystal pins which were originally set flush with the impact surface to measure the flyer velocity as well as the tilt of the impactor. Since the tilt pins are not heated and hence do not thermally expand, their impact time occurs later than the impact with the target assembly. This accounts for the negative time of the first pressure trace and allows additional estimate of the extent of thermal expansion. Plotted to the same time scale in (c) are the pressure profiles recorded by all six gauge stations. These show the initial impact pressure pulse followed by a gradual buildup and eventual transition to

detonation. The last gauge stations was placed at the IHE-aluminum interface and hence the excursion in pressure is due to reflection from an impedance mismatch between aluminum and IHE.

In this case the aluminum flyer velocity was 0.9 mm/μs, but the pressure pulse into the LX-17 sample is only 42 kbar. At ambient temperatures, this pressure would have no effect on the material and would not have caused any reaction resulting in pressure buildup. Here, the transition to detonation took place just prior to the fifth gauge, which, after taking into account axial thermal expansion of 4%, translates into a turnover distance of 12 mm. Because of the thermal expansion of the material and its newly acquired lower density, the detonation parameters of heated LX-17 are also lower than those known to exist under ambient conditions. In our case, detonation pressure of LX-17 at 250°C was about 200 kbar and the detonation velocity was about 6.5 mm/μs. These agree well with the values estimated by empirical means described elsewhere[9], as well as numerical calculations described below.

MODELING

The ignition and growth reactive flow model of shock initiation and detonation of LX-17 has successfully calculated a great deal of one and two dimensional experimental data on LX-17 at ambient temperature,[10, 11] -54°C,[2] and + 88°C.[2] The thermal expansion measurements on LX-17 imply that at 250°C LX-17 and PBX-9502 are approximately 10% porous with a density of approximately 1.7 g/cm^3. Therefore, the unreacted Hugoniot for 250°C IHE must reflect the mechanical properties, such as sound speed, of the hot, porous explosive.

The Jones-Wilkins-Lee (JWL) equation of state which is used for both the unreacted material and the products is written as:

$$P = Ae^{-R_1V} + Be^{-R_2V} + WC_vTV \qquad (4)$$

where P, V, C_V and T are pressure, specific volume, specific heat at constant volume and temperature respectively and A, B, R_1, R_2, and W are constants. The numerical values of all these constants are listed in Table 1.

The unreacted JWL equation of state, that is used in the ignition and growth model, is temperature based so an initial temperature of 523 K is used. To determine the shock velocity and compressibility of hot IHE, embedded manganin pressure gauge records are analyzed from the experiments which were exposed to the lowest shock pressure loadings of 2.5 and 3 GPa. These showed little or no growth of reaction at the shock front at several gauge positions. The shock arrival times at various gauge positions yield accurate shock velocities, and the measured pressures yield shock compressibility data. The unreacted Hugoniat parameters for hot IHE in Table 1 are fitted to these experimental records. The product JWL equation of state in Table 1 is based on thermochemical code and empirical estimations of the differences in detonation properties between 250°C, 1.7 g/cm^3 TATB and 25°C, 1.9 g/cm^3 TATB.

The reaction rate equation of the ignition and growth reactive flow model is of the form:

$$\partial F/\partial t = I(1-F)^b(\rho/\rho_0-1-a)^x + G_1(1-F)^cF^dP^y + G_2(1-F)^cF^gP^z \quad (5)$$

where F is the fraction reacted, ρ is density, P is pressure and I, a, b, x, G_1, c, d, y, G_2, e, g and z are constants. The values of these constants are listed in Table 2. For 250°C, 1.7 g/cm^3 IHE, the first term in Equation (5) representing ignition of "hot spots" created by the shock compression is more important than in ambient temperature, 1.9 g/cm^3 (approximately 2% porous) LX-17 and PBX-9502, because the increased porosity of the heated IHE results in a greater number of heated regions during shock compression. The magnitude of this effect is measured by embedded gauges recording the increases in shock front strengths at greater depths in the shocked explosives. The second term in Equation (5) models the growth of reaction from isolated hot spots into the shocked, heated explosive. This growth rate is much faster than the corresponding rate for ambient IHE, because the hot spots spread more rapidly in the preheated explosive and heated regions.[11] The third term in Equation (5) represents the completion of reaction as detonation is approached. This reaction rate is quite rapid even for ambient TATB and thus is, most likely, not very sensitive to initial temperature.

DISCUSSION OF RESULTS

In the following figures ignition and growth calculations are compared with experimental results. Numerical calculations match all experiments reasonably well with the set of constants which are listed in Table 2.

Figure 5 shows a record that resulted from an impact of an aluminum flyer at 0.81 mm/μs generating a pressure of 30 kb in the LX-17 target. The first gauge which was at an interface between IHE and aluminum buffer saw very little reaction. However, the next two gauges, located 5 and 10 mm deeper into the sample, respectively, showed a drastic increase of reaction with the eventual transition to detonation taking place at or near the fourth gauge originally located 12 mm into the IHE. The last three gauges show a fully developed detonation wave.

Records from another experiment with a stronger impact are shown in Figure 6. The impact velocity of the aluminum flyer onto the aluminum buffer was 0.98 mm/μs, with a pressure pulse into the heated LX-17 of 39 kbar as shown by the first pressure jump at 0.35 μs. The second gauge, located 5 mm into the target, recorded an initial pulse of 50 kbar, followed by a very active chemical reaction that caused the pressure to rise immediately after the shock front. The next gauge that was only 5 mm deeper shows a signal that represents a fully developed detonation wave. Thus, transition to detonation, assuming again the axial thermal expansion of 4%, must have occurred approximately 7.5 mm into the heated sample.

A similar build-up regime is illustrated in Figure 7. Here the explosive is PBX-9502 which is the Los Alamos version of IHE. It contains 2.5% more TATB. The flyer velocity was 0.8 mm/μs and the pressure measured by the first gauge at the buffer-target interface was only 30 kbar. As one can again see at that pressure the first trace remained flat for over 6 μs showing no evidence of any reaction taking place at that interface. The following three gauges registered typical pressure profiles of a regime representing a strong build-up to detonation and finally the last two gauges located originally 16 and 18 mm into the target showed a fully developed detonation

wave. Again, taking into account the proper thermal expansion the run distance to detonation for this system was estimated as 14.5 mm.

Another example with PBX-9502 at a slightly higher impact loading is shown in Figure 8. In this case in addition to a single element manganin gauge in its usual place between the aluminum buffer and the IHE a multi element manganin gauge was placed at the inclined surface of the wedge sample. The target was impacted with an aluminum flyer traveling at a velocity of 0.88 mm/μs. The loading pressure, as measured by the first gauge, was taken as 31 kb. While the first gauge showed no evidence of reaction, throughout the test, the elements of the multimanganin gauge saw consistently rising reaction rates. The transition to detonation probably occurred just behind the last gauge element which again after taking into account thermal expansion of 4% was estimated to be about 15 mm into the heated sample.

Experimental results of all these and other experiments in this series are listed in Table 3. This table also shows calculated values of shock velocity and pressure which one would expect from known equations of state at ambient temperature. Also listed in the table are estimated values of the distances at which the transition to detonation took place. The results do support previous findings[3] that heated IHE does increase in shock sensitivity rather dramatically but still remains less sensitive than HMX based explosives at ambient temperatures. This is best illustrated in Figure 9 on the well known "Pop plot", which shows the run distance to detonation plotted against the impact shock pressure. On this plot the sensitivity is measured by the slope of the curve and its proximity to some already known explosives. The results here are compared with ambient LX-17 and PBX-9404, and they agree well with those obtained at Los Alamos[3].

In all heated experiments the detonation wave pulses are very short, lasting less than 1 μs and do not represent the expected detonation wave profile with the usual Taylor wave expansion. This is probably due to weakening of Teflon armor and consequential failure of small gauge elements under extremely large strains. Under normal conditions thickening of armor prolongs the active life of a gauge element but, at the same time, it reduces the accuracy of the measurement. In the heated environment thickness of the armor may not offer any significant protection because it would also be affected by the heat and weakened by it.

The pressure range covered by the four inch gun experiments is approximately 4 GPa, from 2.5 GPa, where some reaction occurs behind the shock front but transition to detonation does not occur within the 22.5 mm thick hot IHE charge, to approximately 6.5 GPa where the run distance to detonation is 3 mm. The ignition term rapidly reacts up to 10% of the explosive at shock pressures much lower than observed for ambient temperature LX-17, where shock pressures of approximately 6.5 GPa are required to start the initiation process.[10] The subsequent growth of reaction coefficient G_1, for hot IHE in Table 2 is approximately three times that used for ambient LX-17 initiation modeling. This demonstrates the effect of the much higher surrounding temperatures on the growth of the hot spots in these hot IHE experiments.

CONCLUSION

The dynamic experiments provided a significant improvement in our understanding of the problem. However, because of extreme environmental conditions to which the target material is exposed, there is still a lot to be learned about the processes taking place during the event.

The results show that both TATB-based IHE's, LX-17-1 and PBX-9502, at elevated temperatures become significantly more sensitive to shock than they are at ambient temperatures. In fact their shock sensitivity approaches that of an ambient temperature HMX-based explosive such as PBX-9404.

The ignition and growth reactive flow model for hot IHE has been shown to agree reasonably well with embedded gauge records and run distance to detonation data over the pressure regime (2.5-6.5 GPa) studied. Therefore, the model can be reliably used to calculate the effects of more complex hazard scenarios that can not be studied experimentally if these scenarios deal with roughly the same pressure regimes. Model predictions for scenarios involving very different pressure regimes should be used with caution.

ACKNOWLEDGMENTS

The authors wish to express their gratitude to E. L. Lee, L. G. Green and W. C. Tao for their continued interest in this work, to L. Meegan and F. Garcia for their valuable assistance in performing the experiment and to C. Ynzunza for her help with typing of the manuscript. Work performed under the auspices of the U.S. Department of Energy by the Lawrence Livermore National Laboratory under contract No. W-7405-ENG-48.

REFERENCES

1. Scheloske, R., Green, L. , and Weingart, R., Sensitivity of Triaminotrinitrobenzene (TATB) at Elevated Temperatures, UCID-18336, 1980, Lawrence Livermore National Laboratory, Livermore, CA.

2. Urtiew, P. A., Erickson, L. M., Aldis, D. E., and Tarver, C. M., "Shock Initiation of LX-17 as a Function of Its Initial Temperature," Ninth Symposium (International) on Detonation, office of the Chief of Naval Research, OCNR-113291-7, Arlington, VA, 1990, pp. 112-122.

3. Dallman, J. C. and Wackerle, J., "Temperature-Dependent Shock Initiation of TATB-Based High Explosives," This Symposium.

4. Ramsey, J. B. and Popolato, A., "Analysis of Shock Wave and Initiation Data for Solid Explosives," Fourth Symposium (International) on Detonation, ACR-126, Office of Naval Research, 1965, pp. 233-238.

5. Kolb, J. R., and Rizzo, H. F., "Growth of 1, 3, 5-triamino-2,4,6-trinitrobenzene (TATB). I-Anisotropic Thermal Expansion," Propellants and Explosives, Vol. 4, 1979, p.10.

6. Stull, T. W. and Ashcraft, R. W., "Coefficient of thermal expansion of LX-17-1," MHSMP-89-13, Mason & Hanger - Silas Mason Co., Pantex Plant, April 1989.

7. Dobratz, B. and Crawford, P. C., "LLNL Explosives Handbook," UCRL-52997 Change 2, Lawrence Livermore National Laboratory, January 31, 1985.

8. Maienschein, J. L. and Garcia, F., "Thermal expansion of TATB-based explosives from 300 to 520 K," manuscript in preparation.

9. Urtiew, P. A. and Hayes, B., "Emperical Estimate of Detonation Parameters in Condensed Explosives," J. Energetic Materials, 9, No. 4, Nov. 1991, pp. 299-318.

10. Bahl, K., Bloom, G., Erickson, L., Lee, R., Tarver, C., Von Holle, W. and Weingart, R., "Initiation studies on LX-17 Explosives," Eighth Symposium (International) on Detonation, NSWC MP 86-194, Naval Surface Weapons Center, White Oak, Silver Spring, MD, 1986, pp. 1045-1056.

11. Tarver, C. M., "Modeling Shock Initiation and Detonation Divergence Tests on TATB-Based Explosive," Propellants, Explosives, and Pyrotechnics, 15, 1990, p. 132.

12. Dobralz, B. M., Finger, M., Green, L. G., Humphrey, J. R., McGuire, R. R. and Rizzo, H. F., "Selected Sensitivity Tests of Triaminotrinitrobenzene (TATB) Formulation and their Evaluations," Lawrence Livermore National Laboratory, Livermore, CA, UCID-18026 1979.

13. Gibbs, T. R. and Popolato, A., "LASL Explosive Property Data," University of California Press, Berkeley, CA 1980, p. 363.

FIGURE CAPTIONS

Figure 1. Dimensional change in LX-17 pellets when heated to 250-290 C. L/L = axial growth, D/D = radial growth. Data from several runs are shown as grey dots, and 2-nd order polynomial fits are shown as dashed lines.

Figure 2. Measured and reported values for coefficients of thermal expansion for LX-17.

Figure 3. Additional axial expansion in LX-17 pellet held at 250 C for four hours. The expansion during heating to 250 C is not shown in this figure, and L refers to the sample length at the beginning of the isothermal hold time.

Figure 4. Experimental set-up for the 4" gas gun thermal experiment.

Figure 5. Gas gun experiment showing performance of the manganin gauges in an aluminum target at 250 C:
(a) - pressure profiles as recorded by manganin pressure gauges,
(b) - pressure vs particle velocity for symmetrical impact in aluminum.

Figure 6. Gas gun experiment with LX-17 target heated to 250 C.
(a) - target assembly before and after heating with the aluminum flyer just before impact
(b) - distance-time plot showing waves generated by the impact (numbers above lines indicate velocity in mm/us)
(c) - pressure profiles as recorded by manganin pressure gauges.

Figure 7. Pressure profiles in LX-17 heated to 250 C and impacted by an aluminum flyer plate at 0.74 mm/us.

Figure 8. Pressure profiles in LX-17 heated to 250 C and impacted by an aluminum flyer plate at 0.81 mm/us.
(a) - experiment; (b) - computation.

Figure 9. Pressure profiles in LX-17 heated to 250 C and impacted by an aluminum flyer at 0.98 mm/us.
(a) - experiment; (b) - computation.

Figure 10. Pressure profiles in PBX-9502 heated to 250 C and impacted by an aluminum flyer at 0.8 mm/us.
(a) -experiment; (b) - computation.

Figure 11. Pressure profiles in PBX-9502 heated to 250 C and impacted by an aluminum flyer at 0.88 mm/us.
(a) - experiment; (b) - computation.

Figure 12. Run distance to detonation vs impact shock pressure illustrating the sensitivity of heated IHE.

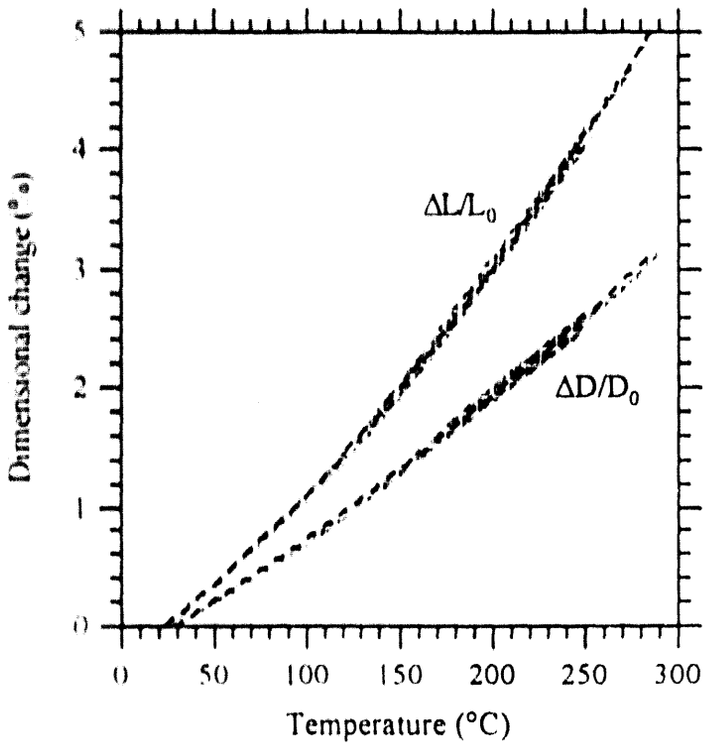
Dimensional change (%)
0
1
2
3
4
5
0
50
100
150
200
250
300
Temperature (°C)
ΔL/L0
ΔD/D0

Fig. 1

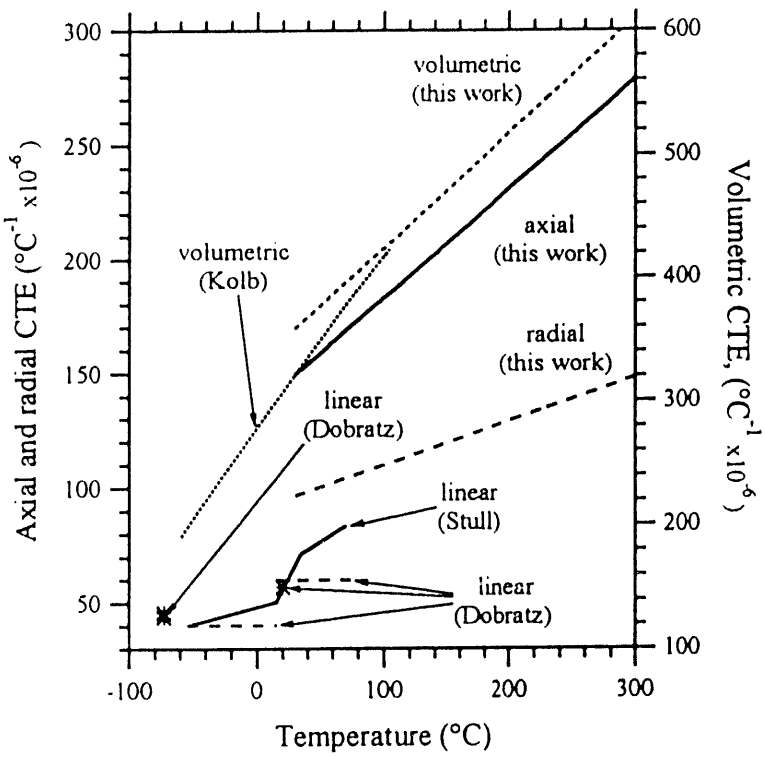
volumetric
(this work)
axial
(this work)
volumetric
(Kolb)
radial
(this work)
linear
(Dobratz)
linear
(Stull)
linear
(Dobratz)
Axial and radial CTE (°C^{-1} x10^{-6})
Volumetric CTE, (°C^{-1} x10^{-6})
Temperature (°C)
300
250
200
150
100
50
600
500
400
300
200
100
-100
0
100
200
300

Fig. 2

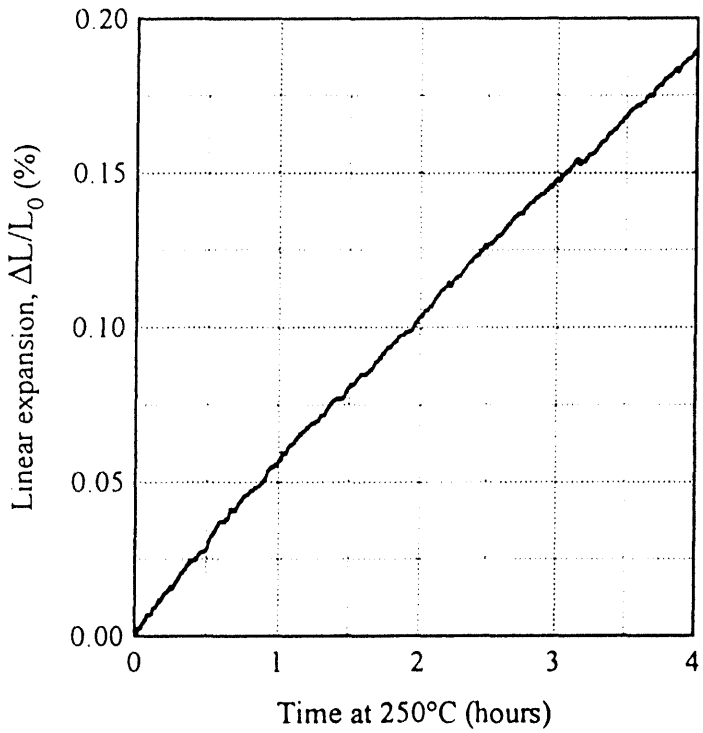
0.20
0.15
0.10
0.05
0.00
Linear expansion, $\Delta L/L_0$ (%)
0
1
2
3
4
Time at 250°C (hours)

Fig. 3

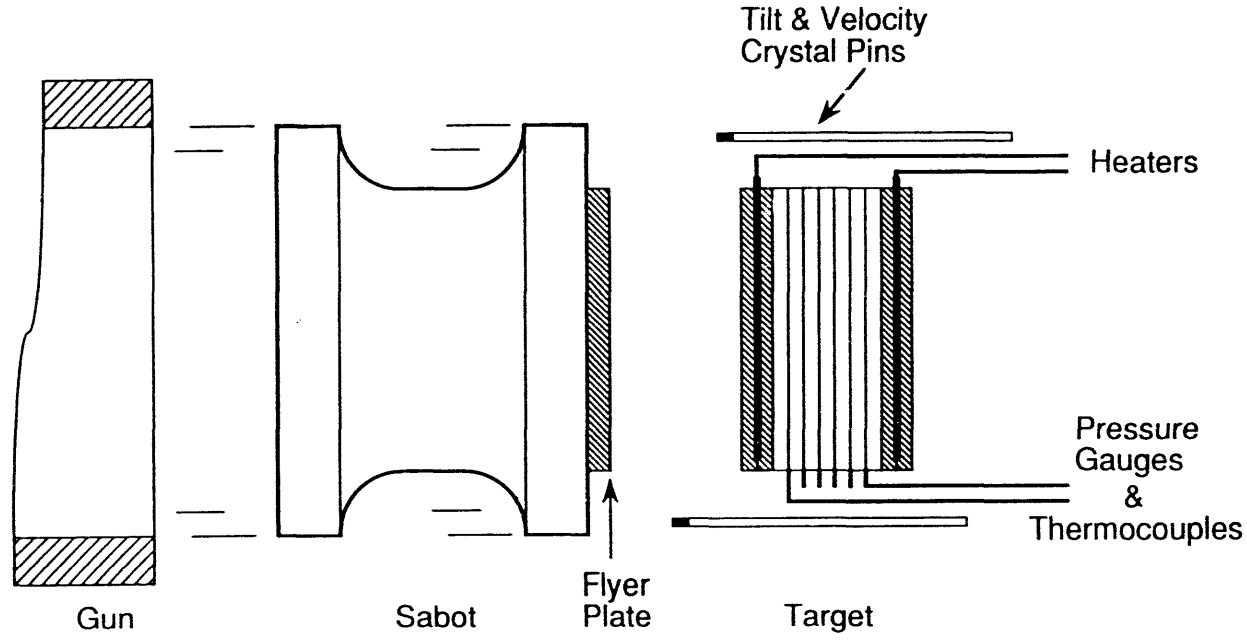
Tilt & Velocity
Crystal Pins
Heaters
Pressure
Gauges
&
Thermocouples
Gun
Sabot
Flyer
Plate
Target

Fig. 4

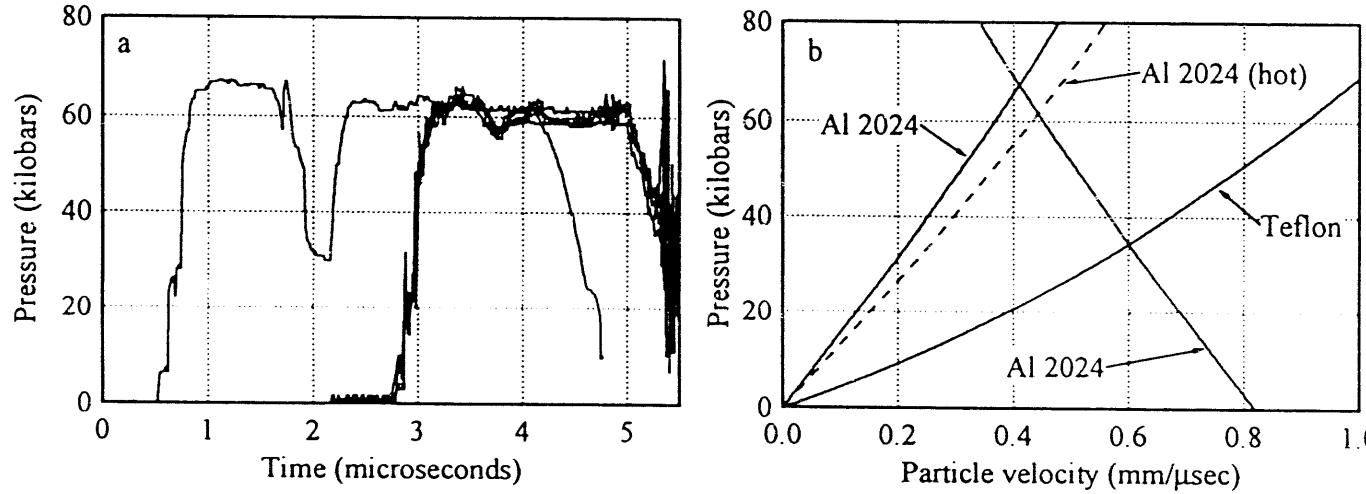

Figure 5 a and b

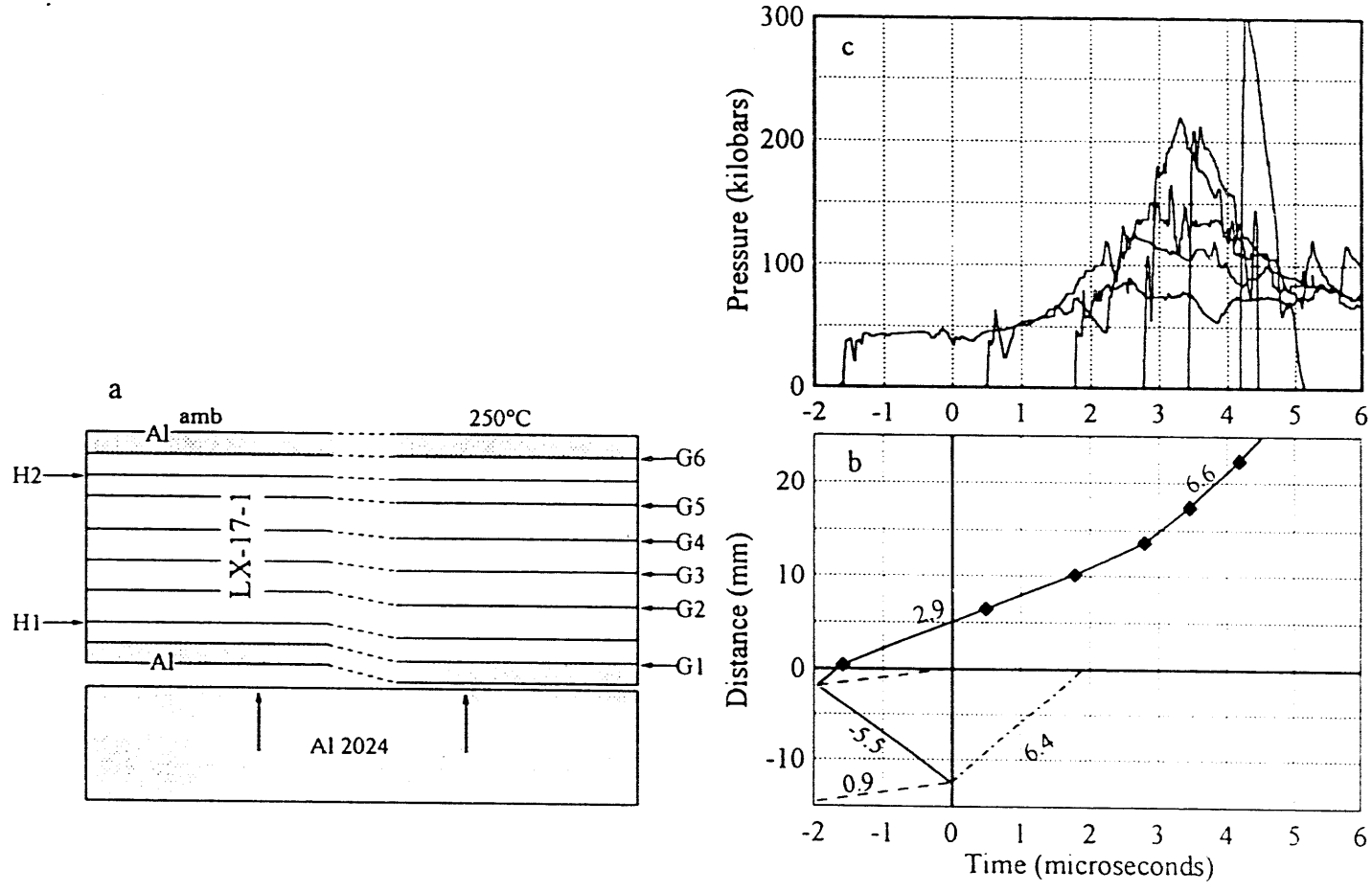
a
amb
250°C
Al
H2
H1
Al
LX-17-1
G6
G5
G4
G3
G2
G1
Al 2024
c
Pressure (kilobars)
300
200
100
0
-2
-1
0
1
2
3
4
5
6
b
Distance (mm)
20
10
0
-10
2.9
6.6
-5.5
0.9
6.4
Time (microseconds)

Figure 6

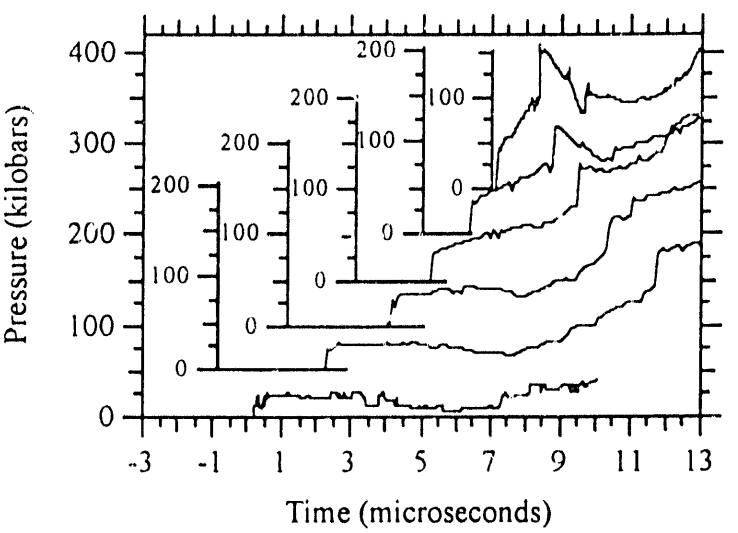
Pressure (kilobars)
400
300
200
100
0
-3
-1
1
3
5
7
9
11
13
Time (microseconds)
200
100
0

Fig. 7

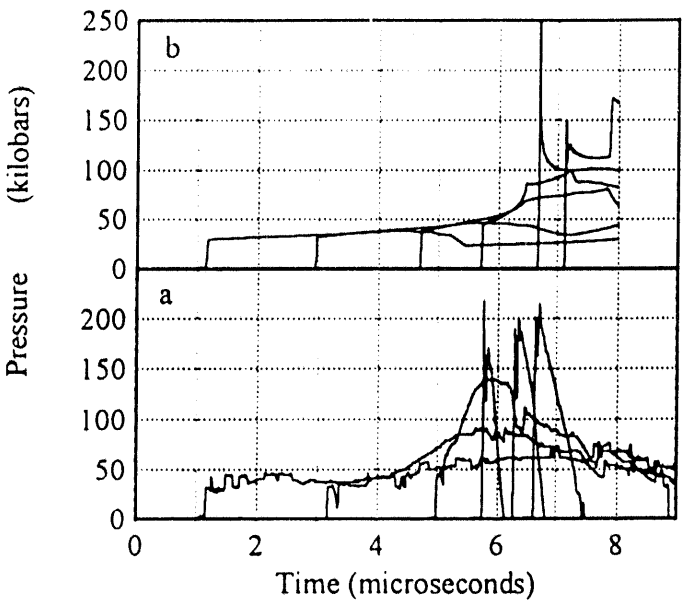
250
200
150
100
50
0
b
a
Pressure (kilobars)
0
2
4
6
8
Time (microseconds)

Figure 8

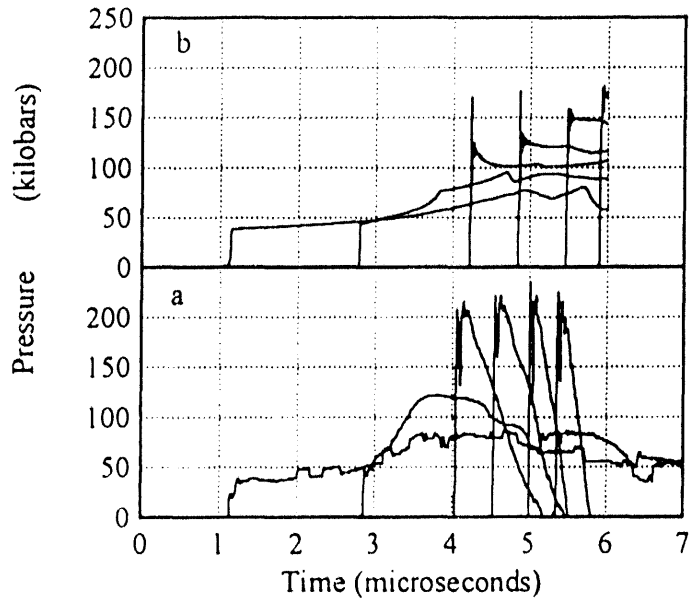
250
200
150
100
50
0
b
a
Pressure (kilobars)
0
1
2
3
4
5
6
7
Time (microseconds)

Figure 9

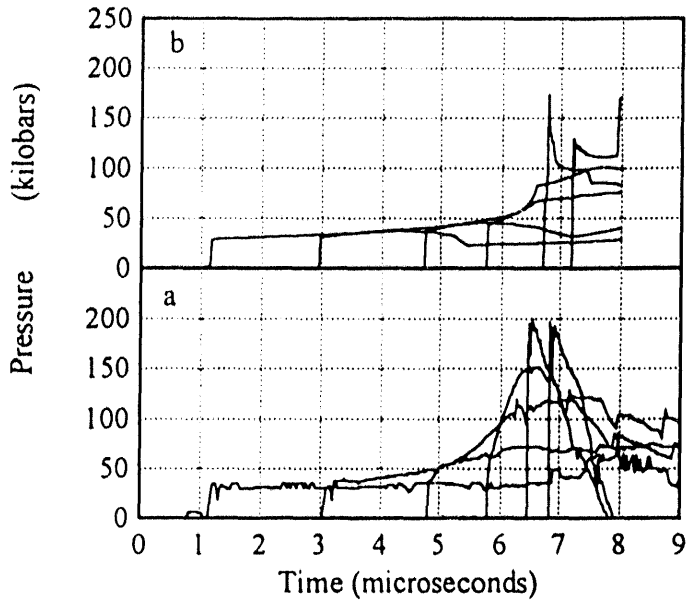
Pressure (kilobars)
250
200
150
100
50
0
b
a
200
150
100
50
0
0 1 2 3 4 5 6 7 8 9
Time (microseconds)

Figure 10

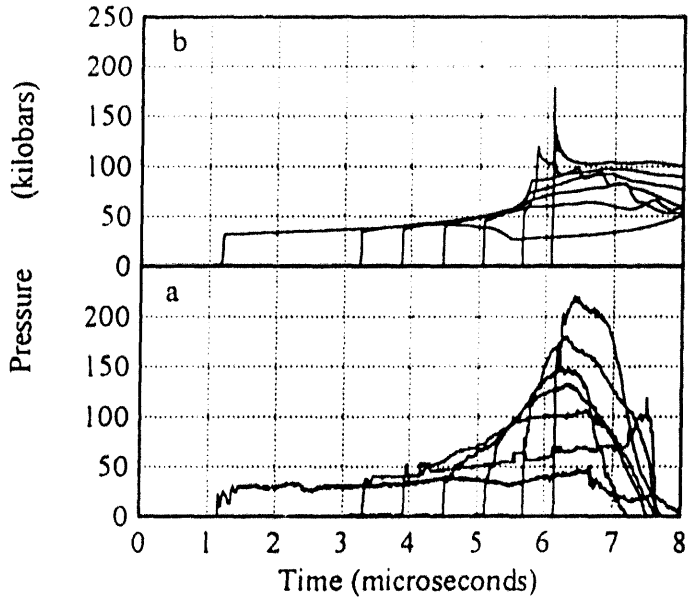
Pressure (kilobars)
250
200
150
100
50
0
b
a
200
150
100
50
0
0 1 2 3 4 5 6 7 8
Time (microseconds)

Figure 11

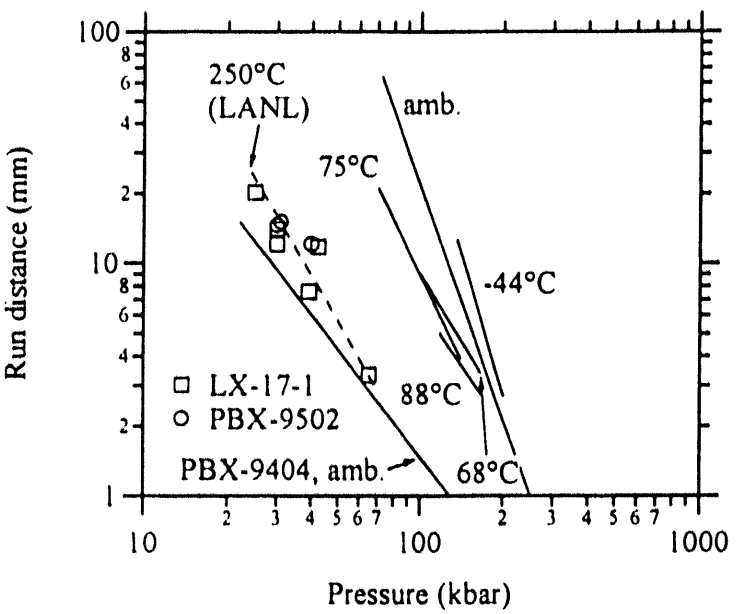
100
10
1
Run distance (mm)
250°C
(LANL)
amb.
75°C
-44°C
88°C
68°C
LX-17-1
PBX-9502
PBX-9404, amb.
10
100
1000
Pressure (kbar)

Figure 12

TABLE 1. JWL EQUATION OF STATE
PARAMETERS FOR MODELING HOT IHE

Parameters	Unreacted	Products
ρ_0 g/cc	1.7	-
A Mbars	244.8	6.5467
B Mbars	-0.0454	0.0712
R_1	11.3	4.45
W	0.894	0.35
Cv Mbars/°K	2.487	1×10^{-5}
T °K	523	-
E_0 Mbars cc/ccg	-	0.062
S Mbars	0.017	-
Y Mbars	0.002	-

TABLE 2. IGNITION AND GROWTH
PARAMETERS FOR MODELING HOT IHE

CONSTANTS					
I	=	$1x10^4$	a	=	0.22
G_1	=	75	b	=	0.667
G_2	=	400.0	c	=	0.667
x	=	7.0	d	=	0.111
y	=	2	e	=	0.333
z	=	3.0	g	=	1.0

LIMITS		
F(I)max	=	0.4
F(G1)max	=	0.5
F(G2) min	=	0.5

TABLE 3. COMPARISON OF EXPERIMENTAL DATA (T_0 = 25°C) WITH CALCULATED VALUES (T_0 = 25°C)

		Calculation (amb)		Experiment 250°		
	Flyer Vel	Us	P	Us	P	run dist.
HE	(mm/μs)	(mm/μs)	(kbar)	(mm/μs)	(kbar)	(mm)
LX-17-1	0.74	3.52	34.4	2.68	25	>20
LX-17-1	0.81	3.64	39.0	2.7	30	12
LX-17-1	0.814	3.63	38.8	2.79	30	14
LX-17-1	0.898	3.77	44.5	3.0	42	11.7
LX-17-1	0.98	3.88	49.0	3.15	39	7.5
LX-17-1	1.295	4.32	70.3	3.5	65	3.3
PBX 9502	0.8	3.62	38.4	2.9	30	14.5
PBX 9502	0.88	3.73	42.76	2.97	31	15
PBX 9502	0.885	3.74	43.0	3.0	40	12

DATE
FILMED
12/7/93
END